Supporting Information

Defective glycerolatocobalt (II) for enhancing oxygen evolution reaction

Junying He, Yuqin Zou*, Shuangyin Wang*

State Key Laboratory of Chemo/Bio-Sensing and Chemometrics, College of Chemistry and Chemical Engineering, Hunan University, Changsha, 410082, P. R.China.

* Corresponding authors.
E-mail: *yuqin_zou@hnu.edu.cn, shuangyinwang@hnu.edu.cn*

Supplementary Index

Experimental Section

1.1 Materials preparation

4 mmol cobalt acetate tetra-hydrate was dissolve into a 100 ml Teflon-lined autoclave containing 50 ml glycerol and was magnetically stirred (500 r/min) for 2 h, and homo-solution was formed, then the reactor was transferred to oven heated to 180℃ and maintained at this temperature for 4 h. After that, the obtained viscous purple mixture was vacuum filtered and washed with ethanol repeatedly until the product was not viscous anymore, the collected purple sample was dried at 60 ℃ for 24 h and ground for spare use. For the Ar plasma treatment, 25 mg sample of CoGly was spread uniformly on the 2 ×3 cm^2 platform of quartz boat, the RF power of 100 W was set, the vacuum degree was controlled at around 13 Pa, and time depending experiments were conducted to obtain the optimized OER performance.

1.2 Characterization

The morphologies and microstructures of the electro-catalysts were observed by scanning

electron microscope (SEM, Hitachi, S-4800) and transmission electron microscope (TEM, JEM-2100, JEOL).Powder X-ray diffraction (XRD) pattern of samples were obtained by using Bruker D8 Advance diffractometer with Cu Kα radiation (operated at 40 kV and 100 mA, λ= 1.54178 Å). X-ray photoelectron spectroscopy (XPS) of sample was performed on a spectrometer (K-Alpha^{+}, Thermo Fisher Scientific) with Al-Kα radiation (1,486.6 eV, pass energy 30.0 eV), the base pressure was controlled around 10^{-9} Torr, and the curve was fitted via standard XPS PEAK 4.1 program. EPR data were obtained on a Bruker EMX X-band spectrometer, and microwave frequency was set as 9.40 GHz at room temperature, light irradiation were measured using a 300W-Xe lamp with a 420 nm cutoff filter.

1.3 Electrochemical Measurement

The catalyst ink was prepared by dispersing 5 mg catalyst into 1 mL mixed solution of ethanol, deionized water and 5% Nafion solution ($V_{ethanol}/V_{water}/V_{Nafion}$=500/450/50), the ink was ultra-sonicated for 20 min before test, then 10 uL ink was dripped on a glassy carbon electrode (5mm in diameter) and was dried under room temperature. All the electrochemical measurements were carried out in a three electrodes system using an electrochemical workstation (CHI 760E, USA). The glassy carbon electrode loaded catalyst was used as working electrode, the graphite rod and saturated calomel electrode (SCE) was used as counter electrode and reference electrode, respectively, 1.0 M KOH was used as electrolyte. The linear scanning voltammetry (LSV) was performed at a scan rate of 5 mV/s to minimize the capacity current, and the electrolyte solution was saturated with O_2 by purging O_2 at the same time. All the polarization curves in this study was corrected by IR compensation, and the obtained potential relative to SCE was calibrated with respect to reversible hydrogen electrode (RHE), the calibration was performed by using Pt wire as working electrode in electrolyte saturated with high purity hydrogen. During the calibration, the CVs were run at a scan rate of 1 mV/s, and the two potentials (hydrogen oxidation and evolution) at current crossing zero were averaged and taken as the thermodynamic potential for hydrogen electrode reaction. So, according to the Nernst equation, in 1 M KOH with pH 13.7, E(RHE)=E(SCE)+1.05.

Under the same three electrodes system, the electrochemical surface area (ECSA) of the working electrode was determined by measuring the capacitive current with double layer charging method, the potential window of theses scan rate dependence of CVs were in the range of no faraday process occurred, the scan rate was set as 5mV/s, 10mV/s, 15mV/s, 20mV/s, and 25mV/s, respectively. The double layer capacitance (C_{dl}) was estimated according to the equation C_{dl} =Ic/ v, Ic is the charging current at median potential, v is the scan rate.

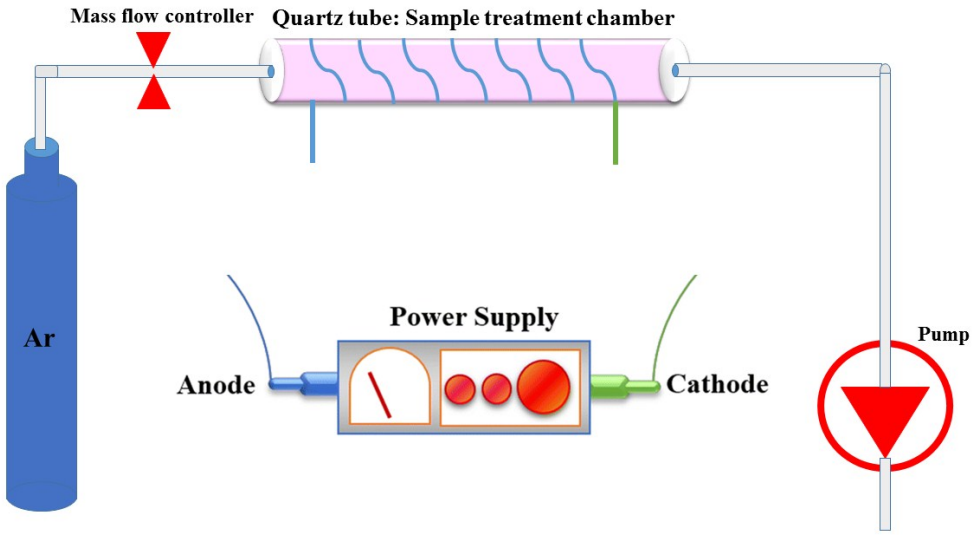

Figure S1. The sketch of plasma equipment used in this experiment.

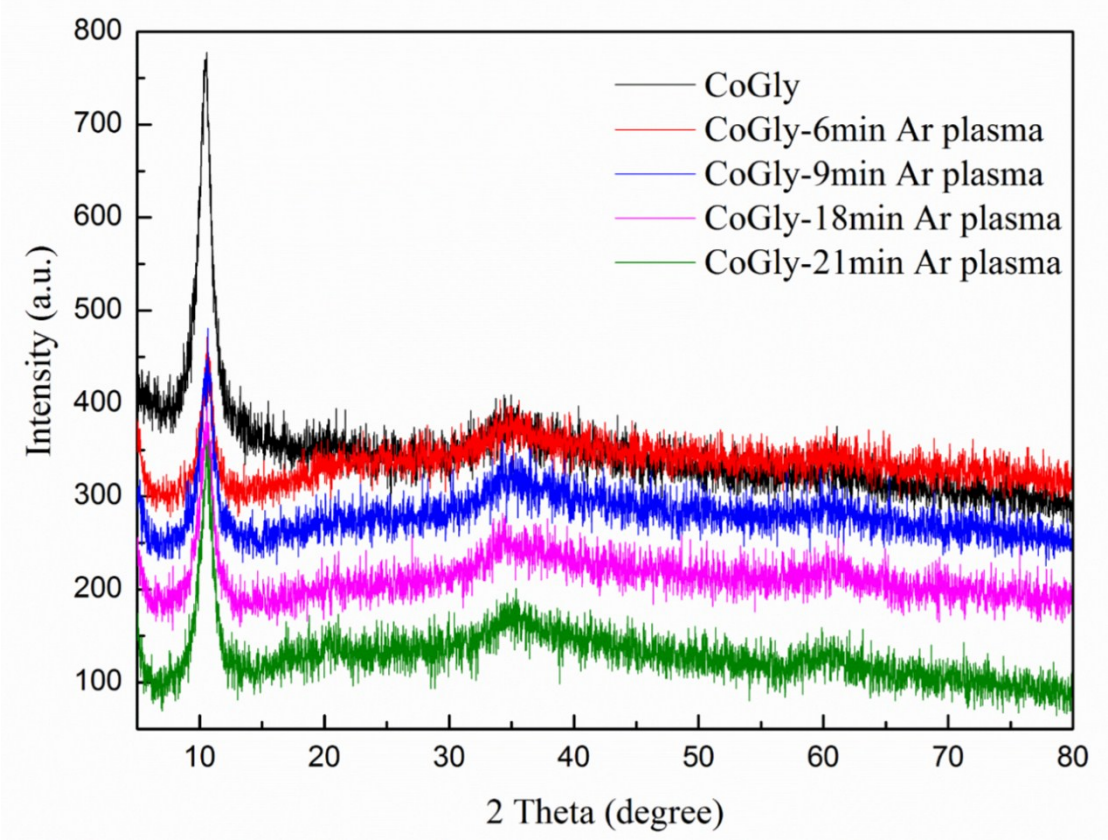

Figure S2. XRD patterns of CoGly treated by Ar plasma for different time.

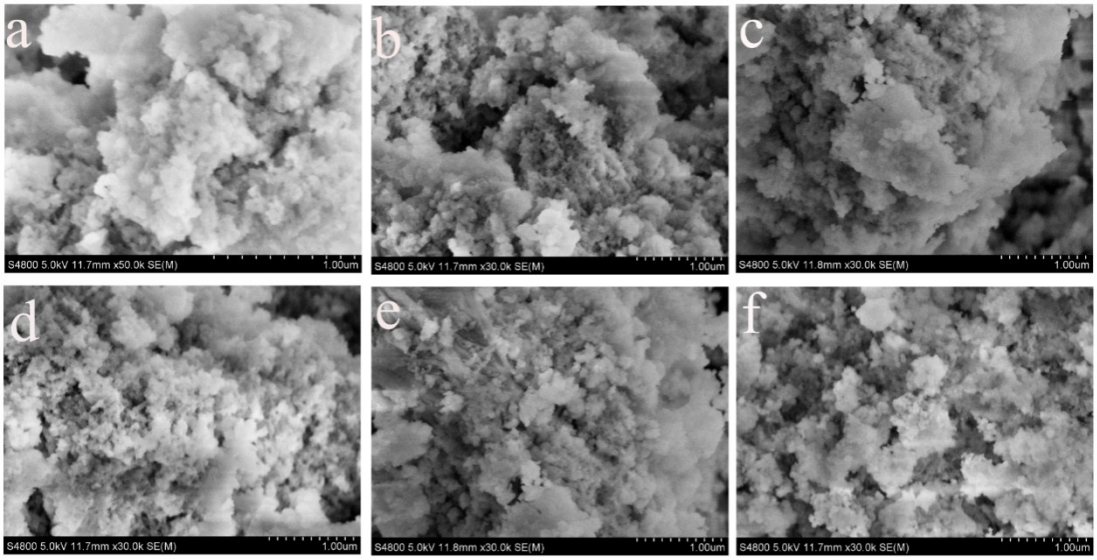

Figure S3. a-f) SEM images of CoGly treated by Ar plasma for 3min, 6min, 9min, 12min, 18min and 21min, respectively.

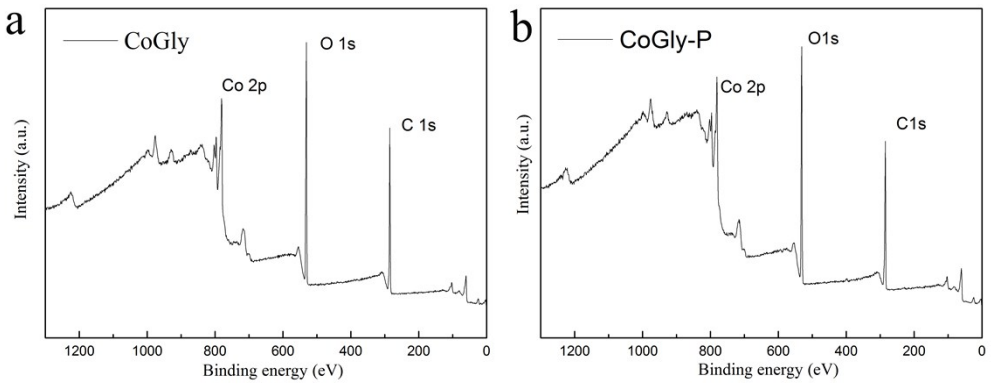

Figure S4. a) XPS survey of CoGly, b) XPS survey of CoGly-P.

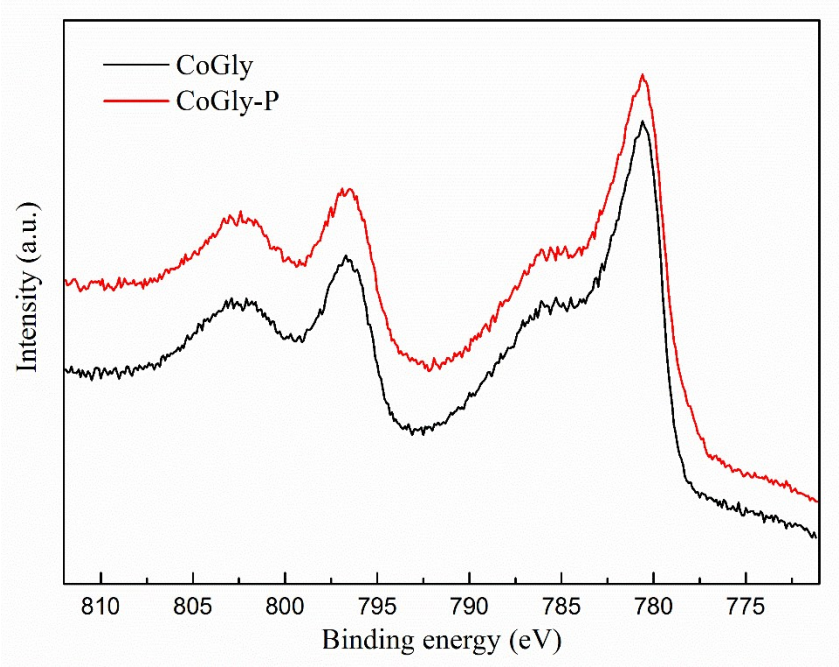

Figure S5. The core line of Co 2p observed from CoGly and CoGly-P

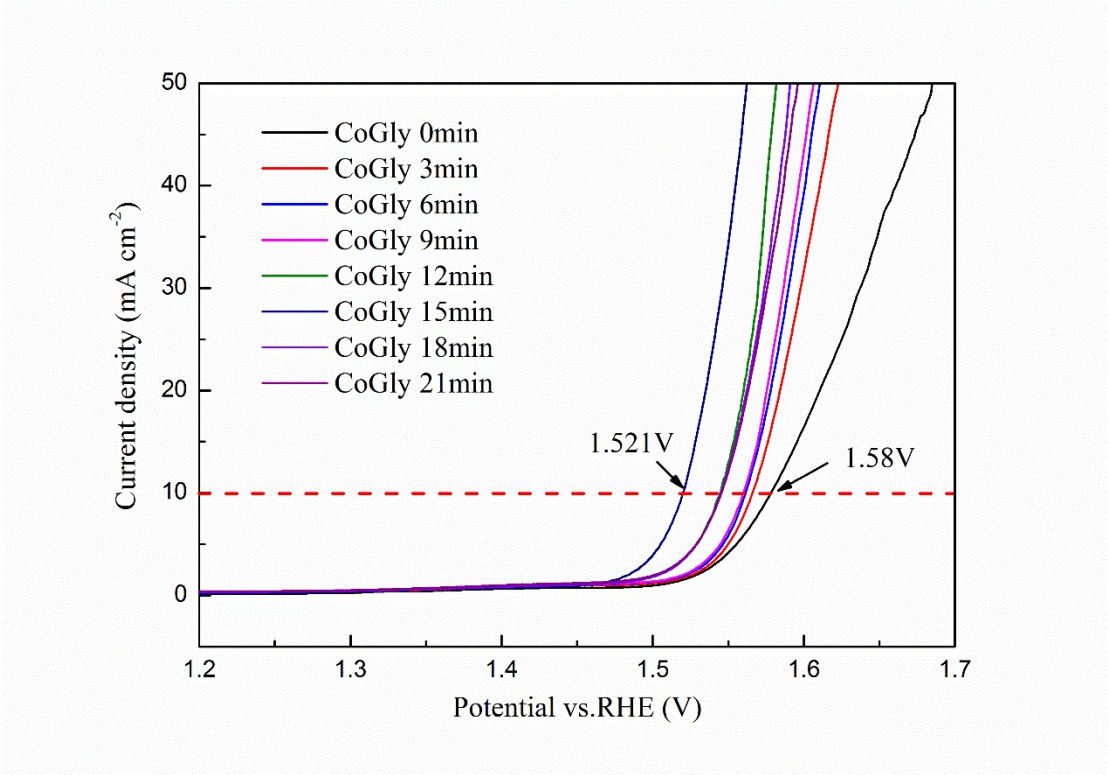

Figure S6. Polarization curves of OER on CoGly treated by Ar plasma for different time.

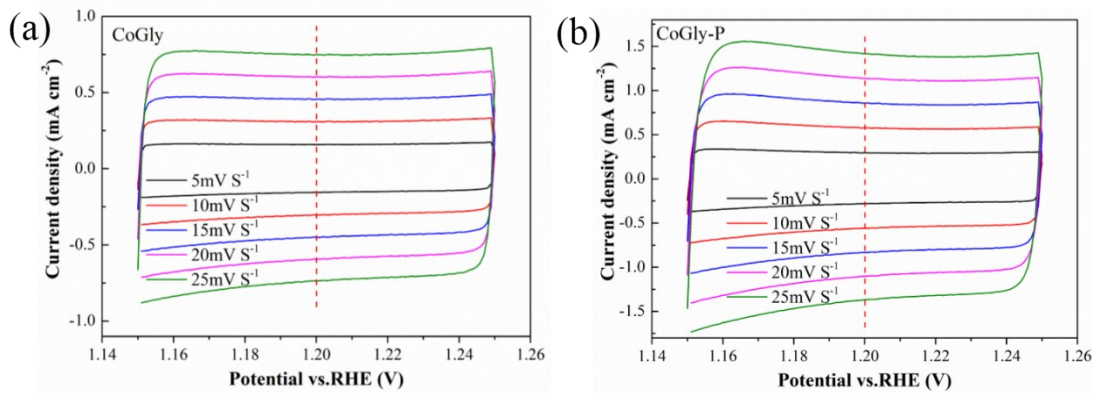

Figure S7. a) CV curves of CoGly under different scanning rates, b) CV curves of CoGly-P under different scanning rates.

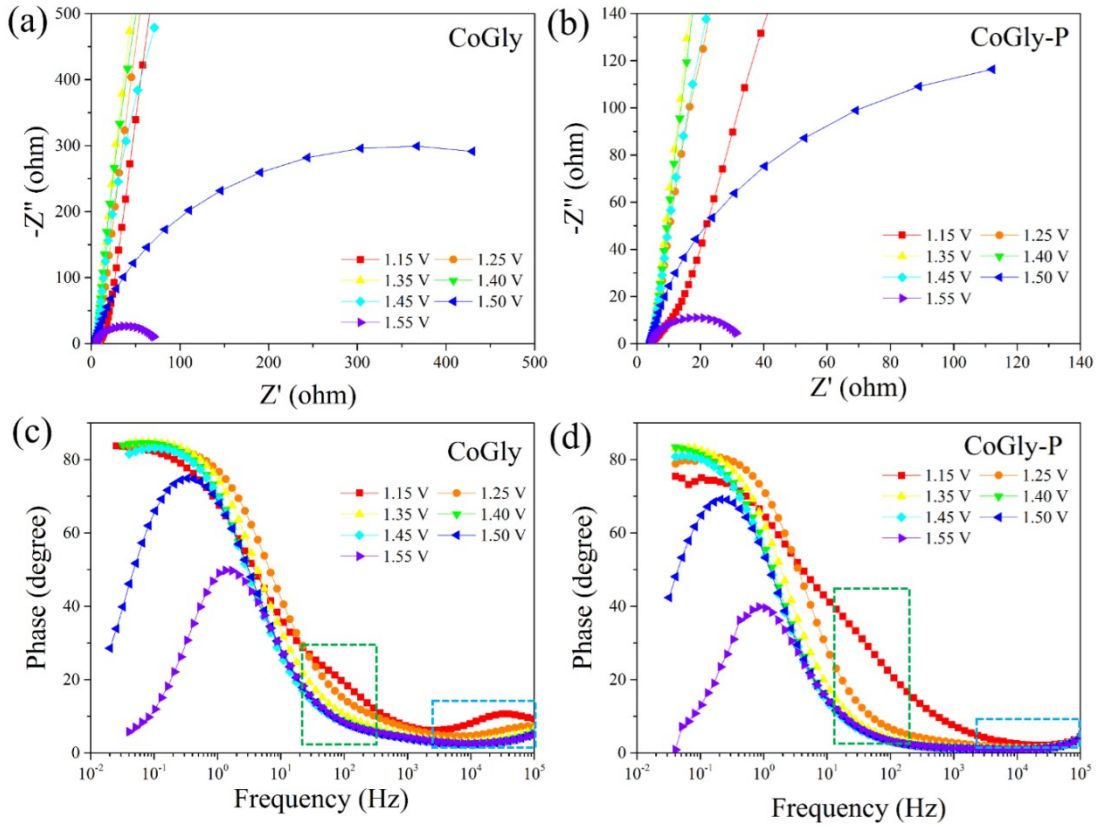

Figure S8. In operando electrochemical impedance spectroscopy (EIS) of CoGly and CoGly-P collected under different polarization potentials (the applied potential is referenced to RHE). a-b) The corresponding Nyquist plots for CoGly and CoGly-P, respectively. c-d) The corresponding Bode-phase plots for CoGly and CoGly-P, respectively.

Table S1: Comparison of OER activities of CoGly-P with other Co-based catalyst and IrO_2.

Electrocatalysts	$\eta_{10mA\ cm^{-2}}$	Tafel slope (mV dec^{-1})	References
CoGly-P	290	56.8	This work
CoGly	350	77.8	This work
α-$Co(OH)_2$ bulk	439	-	1
α-$Co(OH)_2$ Nanosheet	382	107.0	1
α-$Co(OH)_2$ Nano Meshes	303	69.0	1
γ -CoOOH bulk	373	55.0	2
γ -CoOOH NS	300	38.0	2
IrO_2	330	52.0	2
Phy-Co^{2+}	383	91.8	3
P-Phy-Co^{2+}	306	56.2	3
ZIF-67	400	108.8	4
Co_x-ZIF	318	70.3	4
Co-UNMs	307	76.0	5
$Co_{3-x}O_4$	267	38.2	6
2D α-$Co(OH)_2$	267	64.9	7
CoOHCat@NCF	340	38.0	8
O-Co_3O_4	-	49.1	9
Ultrathin 2D Co–MOF nanosheet	263	74.0	10

References

1. B. Zhang, J. Zhang, X. Tan, J. Zhang, *Chem. Commun.*, 2018, **54(32)**, 4045-4048.
2. J. Huang, J. Chen, T. Yao, J. He, S. Jiang, Z. Sun, Q. Liu, W. Cheng, F. Hu, Y. Jiang, Z. Pan and S. Wei, *Angew. Chem., Int. Ed.*, 2015, **54**, 8722-8727
3. D. Yan, C. L. Dong, Y.C. Huang, Y. Zou, C. Xie, Y. Wang, Y. Zhang, D. Liu, S. Shen and S. Wang, *J. Mater. Chem. A*, 2018, **6**, 805-810.
4. S. Dou, C. L. Dong, Z. Hu, Y. C. Huang, J. L. Chen, L. Tao, D. Yan, D. Chen, S. Shen, S. Chou and S. Wang, *Adv. Funct. Mater.*, 2017, **27**, 1702546.
5. Y. Li, F. M. Li, X.Y. Meng, S. N. Li, J. H. Zeng, and Y. Chen, *ACS Catal.*, 2018, **8(3)**, 1913-1920.
6. R. Zhang, W. Xu and J.J. Zou, *ACS Catal.*, 2018, **8**, 3803-3811.
7. Z. Liang, C. Zhang, Y. Xu, W. Zhang, H. Zheng, and R. Cao, *ACS Sustain. Chem. Eng.*, 2018, **7(3)**, 3527-3535.
8. S. Feng, C. Liu, Z. Chai, Q. Li, and D. Xu, *Nano Res.*, 2018, **11(3)**, 1482-1489.
9. Z. Cai, Y. M. Bi, E.Y. Hu, W. Liu, N. Dwarica, Y. Tian, X. L. Li, Y. Kuang, Y. P. Li, X. Q. Yang, H. L. Wang, and X. M. Sun, *Adv. Energy Mater.*, 2018, **8**, 1701694.
10. Y. Xu, B. Li, S. Zheng, P. Wu, J. Zhan, H. Xue, and Pang, H, *J. Mater. Chem. A*, 2018, **6(44)**, 22070-22076.